INSTITUT DE FRANCE
Académie des sciences

Comptes Rendus

Mécanique

Jean Yves Le Pommellec and Adil El Baroudi

Correlation between the toroidal modes of an elastic sphere and the viscosity of liquids

Volume 349, issue 1 (2021), p. 179-188

Published online: 26 March 2021

https://doi.org/10.5802/crmeca.79

This article is licensed under the
Creative Commons Attribution 4.0 International License.
http://creativecommons.org/licenses/by/4.0/

Les Comptes Rendus. Mécanique *sont membres du Centre Mersenne pour l'édition scientifique ouverte*
www.centre-mersenne.org
e-ISSN : 1873-7234

Comptes Rendus
Mécanique
2021, 349, nº 1, p. 179-188
https://doi.org/10.5802/crmeca.79

Short paper / *Note*

Correlation between the toroidal modes of an elastic sphere and the viscosity of liquids

Jean Yves Le Pommellec [a] **and Adil El Baroudi** [a] *

[a] Arts et Metiers Institute of Technology, Angers, France

E-mails: jeanyves.lepommellec@ensam.eu (J. Y. Le Pommellec), adil.elbaroudi@ensam.eu (A. El Baroudi)

Abstract. Vibration characteristics of elastic nanostructures embedded in fluid medium have been used for biological and mechanical sensing and also to investigate materials and mechanical properties. An analytical approach has been developed in this paper to accurately predict toroidal vibrations of an elastic nanosphere in water–glycerol mixture. The Maxwell and Kelvin–Voigt models are used to describe the viscoelasticity of this fluid. The influence of key parameters such as glycerol mass fraction, sphere radius, and angular mode number are studied. We demonstrate that the sphere radius plays a significant role on the quality factor. Results also highlight three behavior zones: viscous fluid, transition, and elastic solid. In addition, these investigations can serve as benchmark solution in design of liquid sensors.

Keywords. Viscoelastic liquid, Elastic sphere, Toroidal vibration, Analytical approach, Maxwell model, Kelvin–Voigt model.

Manuscript received 23rd December 2020, revised 11th March 2021, accepted 12th March 2021.

1. Introduction

Vibration analysis of embedded nanoparticles in fluid medium have attracted strong interest owing to various applications, especially in designing biological sensors [1–6]. In addition, incited by the idea to destroy biological nanoparticles such as viruses, the elastic sphere model was also used to study the vibration characteristics of viruses in different media [7–11]. The experimental study of the damping mechanism and resonant frequencies of these nanoparticles have been measured by experimental techniques [5, 12, 13]. The vibrations of spherical particles were studied a century ago by Lamb [14]. Two types of modes, spheroidal and toroidal, are derived from the stress-free boundary condition of a spherical surface. Theoretical studies were recently developed for predicting the various vibration scenarios of a gold nanosphere in water–glycerol mixture [15–18]. In these papers, the Maxwell model is used to describe the viscoelasticity of the

* Corresponding author.

fluid. A novel analytical approach using Maxwell and Kelvin–Voigt models is proposed in this paper for predicting the toroidal vibrations of an elastic sphere in water–glycerol mixture. Furthermore, the concept of toroidal mode dipstick is attractive in industry for fluid characterizations. The idea is that the toroidal mode of an elastic structure can sense the fluid rheological properties. The toroidal mode of the structure interacts with fluid boundary, it follows that the toroidal mode properties are highly affected [19–21]. Moreover, the metallic nanospheres whose volume and shape do not change, vibrate toroidally.

2. Viscoelastic fluid mathematical formulation

To describe the viscoelasticity of the fluid, the Maxwell and Kelvin–Voigt models are employed. The Maxwell model introduces the viscoelastic response of the fluid at high frequencies and that of Kelvin–Voigt at low frequencies. The Maxwell model consists of a spring and a damper connected in series, and for the Kelvin–Voigt model, the spring and the damper are connected parallel. The damper represents energy losses and is characterized by the viscosity η, whereas the spring represents the energy storage and is characterized by the elastic shear modulus μ. These two quantities are related through the relaxation time $\delta = \eta/\mu$, which is the characteristic time for the transition between viscous and elastic behavior [22]. Thus, suppose the motion of the fluid is induced only by elastic sphere vibration. In regard to this problem, the inertial term in the Cauchy's equation can be omitted. Therefore, the governing equation for the fluid is simplified as follows:

$$\rho_f \frac{\partial \mathbf{v}}{\partial t} = \nabla \cdot \boldsymbol{\tau}, \tag{1}$$

where ρ_f is the density and $\mathbf{v}$ is the velocity vector. For an incompressible Newtonian liquid, $\boldsymbol{\tau}$ is the shear stress tensor, and which is related to the deformation by the following constitutive equation

$$\boldsymbol{\tau} = 2\eta \mathbf{D}, \tag{2}$$

where η is the shear viscosity and $\mathbf{D} = [\nabla \mathbf{v} + (\nabla \mathbf{v})^T]/2$ is the strain rate tensor. The standard Newtonian constitutive equation (2) is easily generalized to account for the shear relaxation behavior of a linear viscoelastic fluid. Considering the physical model of Maxwell and Kelvin–Voigt, immediately leads to the following generalization

$$\delta \frac{\partial \boldsymbol{\tau}}{\partial t} + \boldsymbol{\tau} = 2\eta \mathbf{D} \tag{3}$$

$$\frac{\partial \boldsymbol{\tau}}{\partial t} = 2\mu \mathbf{D} + 2\eta \frac{\partial \mathbf{D}}{\partial t}. \tag{4}$$

The stress–strain relation (3) is suggested by Maxwell for the characterization of viscous fluids with elastic properties, and the stress–strain relation (4) is proposed by Kelvin–Voigt for the description of elastic solids with viscous properties. Also, Equations (3) and (4) take into accounts for shear relaxation effect, while giving a purely Newtonian result in the low (or high) frequency limit and a purely elastic response in the corresponding high (or low) frequency limit.

Since toroidal vibration is assumed, we utilize a spherical coordinate system located at the center of the sphere. Vibrations of first class or toroidal vibrations [14] are characterized by the absence of displacement in the radial direction, and is purely an equivoluminal motion. Therefore, the pertinent velocity field of the fluid, $\mathbf{v}(r, \theta, \varphi, t) = v_\theta(r, \theta, \varphi, t)\mathbf{e}_\theta$, have only circumferential component, where r is the usual radial coordinate in spherical coordinates, θ is the inclination, φ is the azimuth, t is the time, and e_θ is its corresponding basis vector. Applying the divergence operator to both sides of (3) and (4), and taking into account the equation of motion (1), we get

the following viscoelastic fluid equation expressed in terms of the circumferential component of the velocity field

$$\nabla^2 v_\theta - \frac{v_\theta}{r^2 \sin^2\theta} - \frac{\rho_f}{\eta}\left(1+\delta\frac{\partial}{\partial t}\right)\frac{\partial v_\theta}{\partial t} = 0 \tag{5}$$

$$\left(1+\delta\frac{\partial}{\partial t}\right)\left(\nabla^2 v_\theta - \frac{v_\theta}{r^2\sin^2\theta}\right) - \frac{\rho_f}{\mu}\frac{\partial^2 v_\theta}{\partial t^2} = 0. \tag{6}$$

Equation (5) describes the fluid motion according to the Maxwell behavior and (6) to that of Kelvin–Voigt behavior. Use of (5) and (6) together with the appropriate fluid boundary conditions, allows for characterization of the viscoelastic response of simple fluids. Throughout, we assume the time-harmonic dependence of $e^{j\omega t}$ for all variables, where ω is the angular frequency. Then, Equations (5) and (6) can be expressed in the form

$$\frac{\partial}{\partial r}\left(r^2\frac{\partial v_\theta}{\partial r}\right) + \frac{1}{\sin\theta}\frac{\partial}{\partial\theta}\left(\sin\theta\frac{\partial v_\theta}{\partial\theta}\right) + \frac{1}{\sin^2\theta}\frac{\partial^2 v_\theta}{\partial\varphi^2} - \frac{v_\theta}{\sin^2\theta} - \frac{j\omega\rho_f}{\eta^*}r^2 v_\theta = 0, \tag{7}$$

where the dynamic complex viscosity η^* is given according to the used viscoelastic fluid behavior as

$$\eta^* = \begin{cases} \dfrac{\eta}{1+j\omega\delta} & \text{for Maxwell fluid} \\ \eta + \dfrac{\eta}{j\omega\delta} & \text{for Kelvin–Voigt fluid.} \end{cases} \tag{8}$$

Using previously developed techniques [23], Equation (7) can be solved to yield

$$v_\theta = \sum_{n=0}^{\infty}\sum_{m=-n}^{n}\sqrt{\frac{\pi}{2k_f r}}\left[AI_{n+\frac{1}{2}}(k_f r) + BK_{n+\frac{1}{2}}(k_f r)\right]P_n^m(\cos\theta)\cos(m\varphi), \tag{9}$$

where $k_f = \sqrt{j\omega\rho_f/\eta^*}$, A and B are arbitrary constants, $I_{n+1/2}(k_f r)$ and $K_{n+1/2}(k_f r)$ are modified spherical Bessel functions of the first and second kind, $P_n^m(\cos\theta)$ are associated Legendre polynomials. The integers m and n are the azimuthal and angular dependences of the toroidal vibration mode, respectively. Note that the time factor $e^{j\omega t}$ is omitted for simplicity. In addition, the circumferential component of stress tensor that will be used later in boundary conditions can be written as

$$\tau_{r\theta} = \eta^*\left(\frac{\partial v_\theta}{\partial r} - \frac{v_\theta}{r}\right). \tag{10}$$

3. Elastic sphere mathematical formulation

In this section, the constitutive equations for a viscoelastic fluid in (3) and (4) are used to examine the fluid–structure interaction of a spherical particle executing toroidal vibration in a fluid. This solution finds direct application in practice, because these particles are measured using ultrafast laser spectroscopy to probe their dynamics [5, 24, 25]. Therefore, it has been established that nanometer-sized solid particles obey the continuum hypothesis [6,26] with their dynamics being governed by Navier's equation

$$\frac{\partial^2\mathbf{u}}{\partial t^2} = c_s^2\left(\nabla^2\mathbf{u} - \nabla\nabla\cdot\mathbf{u}\right) + c_c^2\nabla\nabla\cdot\mathbf{u}, \tag{11}$$

where $\mathbf{u}$ is the displacement field, c_c and c_s are the propagation velocities of compressional and shear waves in the elastic sphere, respectively. An analytical solution can be found for the toroidal mode of a sphere vibrating in a viscoelastic fluid. Throughout, we assume that the solid particle undergoes small-amplitude oscillations, and thus the usual assumption of linear elasticity is applicable. Note again that the toroidal mode exhibits a pure circumferential displacement, that is, $\mathbf{u}(r,\theta,\varphi,t) = u_\theta(r,\theta,\varphi,t)\mathbf{e}_\theta$. The time-harmonic dependence for all variables with the same

vibration frequencies of the viscoelastic fluid is assumed. Therefore, the governing equation for the circumferential displacement of a sphere (11) becomes

$$\frac{1}{r^2}\frac{\partial}{\partial r}\left(r^2\frac{\partial u_\theta}{\partial r}\right)+\frac{1}{r^2\sin\theta}\frac{\partial}{\partial\theta}\left(\sin\theta\frac{\partial u_\theta}{\partial\theta}\right)+\frac{1}{r^2\sin^2\theta}\frac{\partial^2 u_\theta}{\partial\varphi^2}+\frac{\omega^2}{c_s^2}u_\theta=0. \tag{12}$$

In a similar manner that fluid velocity, is easily to show that the elastic sphere displacement given in (12) can be expressed as follow

$$u_\theta=\sum_{n=0}^{\infty}\sum_{m=-n}^{n}\sqrt{\frac{\pi}{2k_s r}}CJ_{n+\frac{1}{2}}(k_s r)\cos(m\varphi)P_n^m(\cos\theta), \tag{13}$$

where C is an arbitrary constant, $J_{n+1/2}(k_s r)$ is the spherical Bessel functions of the first kind, and $k_s=\omega/c_s$ is the shear wavenumber. Also, according to the generalized linear Hooke's law, the circumferential component of stress tensor that will further be used in boundary condition is expressed as

$$\sigma_{r\theta}=\rho_s c_s^2\left(\frac{\partial u_\theta}{\partial r}-\frac{u_\theta}{r}\right), \tag{14}$$

where ρ_s is the solid density.

4. Sphere–fluid interaction and eigenvalue equation

The vibration frequencies of the coupled system shall be obtained by application of the appropriate boundary conditions. Therefore, the following relations are suitable: (i) flux continuity that describes mass conservation and equilibrium of the normal forces at the sphere–fluid interface

$$v_\theta=\mathrm{j}\omega u_\theta,\quad \tau_{r\theta}=\sigma_{r\theta}. \tag{15}$$

(ii) The nonslip boundary condition for the outside surface of viscoelastic fluid is assumed

$$v_\theta=0. \tag{16}$$

Equations (15) and (16) show the boundary and interface conditions between viscoelastic fluid and elastic sphere. Substitution of (9) and (13) into these boundary conditions and taking into account the Equations (10) and (14), provides three linear and homogeneous equations for the arbitrary constants A, B, and C. This system of equations has a nontrivial solution if the determinant of the coefficients equals zero. This leads to the following complex eigenvalue equation

$$\frac{I_{n+\frac{1}{2}}(k_f b)K_{n+\frac{3}{2}}(k_f a)+K_{n+\frac{1}{2}}(k_f b)I_{n+\frac{3}{2}}(k_f a)}{I_{n+\frac{1}{2}}(k_f b)K_{n+\frac{1}{2}}(k_f a)-K_{n+\frac{1}{2}}(k_f b)I_{n+\frac{1}{2}}(k_f a)}+\frac{\mathrm{j}\rho_s c_s}{k_f\eta^*}\left[\frac{J_{n+\frac{3}{2}}(k_s a)}{J_{n+\frac{1}{2}}(k_s a)}-\frac{n-1}{k_s a}\left(1-\frac{\mathrm{j}k_s\eta^*}{\rho_s c_s}\right)\right]=0. \tag{17}$$

Complex eigenvalue equation (17) constitute an implicit transcendental function of n and ω. The roots ω may be computed for a fixed n. It is interesting to note that this complex eigenvalue equation is independent of the values of m. This arises as a consequence of the presence of spherical symmetry. Moreover, in the case of an elastic sphere vibrating in vacuum, eigenvalue equation (17) becomes

$$J_{n+\frac{3}{2}}(k_s a)-\frac{n-1}{k_s a}J_{n+\frac{1}{2}}(k_s a)=0 \tag{18}$$

which was previously obtained by Lamb [14].

Table 1. Fluid properties for different glycerol mass fractions χ

χ	0	0.36	0.56	0.71	0.80	0.85
ρ_f (kg/m^3)	1000	1090	1140	1190	1210	1220
η (mPa·s)	0.894	2.7	5.27	20	44.7	92.3
δ (ps)	0.647	1.87	3.51	12.7	27.1	54.2

5. Results and discussion

In this paragraph, the numerical calculations for a gold nanosphere submerged in a viscoelastic fluid are conducted in order to quantitatively investigate the fluid model effect on the vibration characteristics of the fluid–structure interaction system.

Due to the presence of a damping mechanism, the angular frequency can be written as $\omega = \omega_r + \mathrm{j}\omega_i$ with ω_r and ω_i are, respectively, the real and imaginary parts of the angular frequency. In this paper, the quality factor $Q = \sqrt{\omega_r^2 + \omega_i^2}/(2\omega_i)$ which is a scaled rate of energy dissipation, and is defined as the ratio of the maximum energy stored, in the particle to the energy dissipated per cycle [15, 16]. In addition, the vibration frequency means the real part of the frequency and is defined as $f = \omega_r/(2\pi)$. Furthermore, it should be mentioned that, since the complex eigenvalue equation (17) are derived for three-dimensional motions, there exist an infinite number of eigenvalues for each angular mode number n.

The material properties given in Table 1 for viscoelastic fluid and which are used by Galstyan *et al.* [15] were taken to construct this numerical example. The density $\rho_s = 19{,}700$ kg/m^3 and the propagation velocity of shear waves in the gold nanosphere $c_s = 1200$ m/s used in this work were also derived from Galstyan *et al.* [15].

Table 2 shows the first ten natural toroidal frequencies and quality factors of a gold nanosphere in a water–glycerol mixture with $\chi = 0.56$. It is seen that for each model (Kelvin–Voigt, Maxwell, Newtonian) the lowest frequency value is obtained for $n = 2$ (lowest frequency). This mode is called fundamental toroidal mode. Otherwise for a fixed n, the quality factor increases (and the damping decreases) with frequency. On the other hand, the calculated frequency does not depend on the used model and remains closed to the values obtained by Lamb for a sphere in vacuum. Therefore, the frequency is not very sensitive to the surrounding liquid (see Figure 5). On the contrary the quality factor values depend strongly on the model and on the viscoelastic properties of the medium. In addition, the modes in Table 2 are not in order with the parameters n and l. For example, the frequency of mode $(4, 1)$ is lower than that of mode $(1, 1)$. Therefore, one should be careful to find the right mode of the vibration.

5.1. *Influence of the glycerol mass fraction*

In this paragraph, we investigate how the quality factor of the fundamental toroidal mode ($n = 2$) varies with the glycerol mass fraction in both Newtonian and viscoelastic fluids. Three radius are taken into account: $a = 40$ nm (Figure 1(a)); $a = 20$ nm (Figure 1(b)); and $a = 10$ nm (Figure 1(c)). In Figure 1, by increasing the glycerol mass fraction, Newtonian and Kelvin–Voigt models predicted a monotonically decreasing relationship between the quality factor and the glycerol mass fraction. However, Maxwell mode highlighted a nonmonotonically behavior which manifested the intrinsic viscoelastic properties of fluid. A pair of critical glycerol mass fractions (0.56, 0.71) is highlighted for a gold nanosphere radius equal to 40 nm (Figure 1(a)). It is seen that the Newtonian curve converge to the Maxwell one for $\chi < 0.56$ and to Kelvin–Voigt one for $\chi > 0.71$. For $\chi < 0.56$, the water–glycerol mixture behaves as a viscoelastic liquid, and for $\chi > 0.71$, the mixture behaves as a viscoelastic solid. A transition zone appears for $0.56 < \chi < 0.71$. In this

Table 2. Quality factor and vibration frequency of the gold nanosphere with 20 (nm) radius vibrating in water–glycerol mixture with $\chi = 0.56$

		Kelvin–Voigt		Maxwell		Newtonian		
n	l	Q	f (GHz)	Q	f (GHz)	Q	f (GHz)	f_{Lamb} (GHz)
2	1	7.166	25.077	8.674	23.755	7.976	23.213	23.884
3	1	8.957	37.766	12.068	36.950	9.358	36.070	36.905
4	1	9.900	49.404	15.214	48.831	9.875	47.699	48.649
1	1	34.335	54.930	53.034	54.983	44.383	54.625	55.036
5	1	10.349	60.566	18.297	60.116	10.011	58.802	59.933
2	2	37.659	67.977	60.883	68.109	45.526	67.665	68.143
6	1	10.499	71.458	21.333	71.056	9.954	69.614	70.699
3	2	39.583	80.437	68.240	80.624	45.522	80.107	80.643
7	1	10.470	82.179	24.315	81.772	9.794	80.247	81.358
1	2	49.990	86.557	82.600	86.816	60.020	86.333	86.850

l describes the harmonic number.

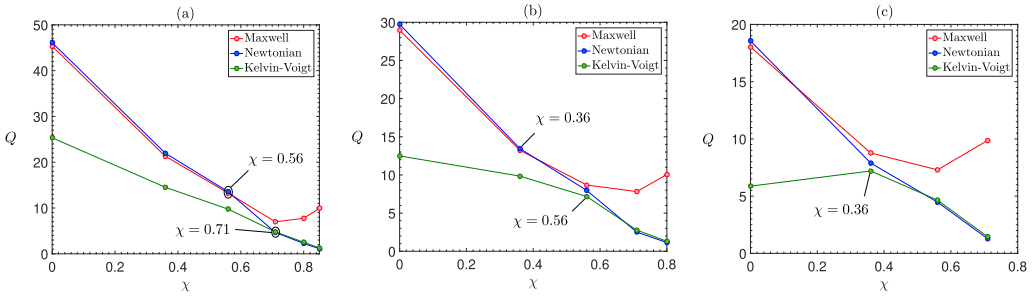

Figure 1. Quality factor versus glycerol mass fraction. (a) For $a = 40$ nm, (b) for $a = 20$ nm, and (c) for $a = 10$ nm.

range of glycerol mass fraction the quality factor values calculated with Newtonian, Maxwell and Kelvin–Voigt models are different. The same behavior is observed if $a = 20$ nm (Figure 1(b)). In this case, the pair of critical values is (0.36, 0.56). The water–glycerol mixture behaves as a viscous liquid for $\chi < 0.36$ and as an elastic solid for $\chi > 0.56$. The transition zone observed for $0.36 < \chi < 0.56$ is shifted to the left if the sphere radius decreases from $a = 40$ nm to $a = 20$ nm. If the sphere radius decreases to 10 nm (Figure 1(c)), the convergence between Maxwell and Newton curves are not observed. Otherwise, the Kelvin–Voigt and Newton curves converge for $\chi > 0.36$. For $\chi < 0.36$, the quality factor values calculated with Newtonian, Maxwell and Kelvin–Voigt models are different. These values correspond to the transition zone which is shifted toward left when the sphere radius decreases from 20 nm to 10 nm. Consequently, for low sphere radius (10 nm) the water–glycerol mixture behaves as an elastic solid.

5.2. *Influence of the sphere radius*

In this paragraph, we investigate how the sphere radius influences the variation of the quality factor. Figure 2 illustrates the sphere radius effect on the quality factor for three glycerol mass fraction ($\chi = 0, 0.56, 0.71$). The predicted quality factor by the Newtonian and Kelvin–Voigt models increases with increasing radius. This is due to the decreasing of the damping component as the radius increases. A nonmonotonic variations of the quality factor with the radius is observed for

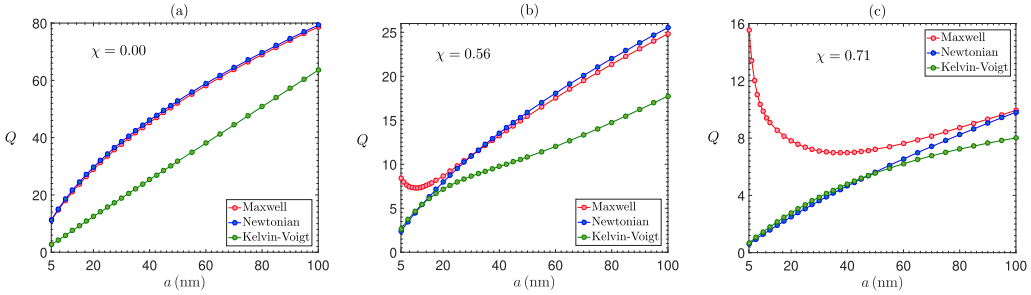

Figure 2. Quality factor versus nanosphere radius.

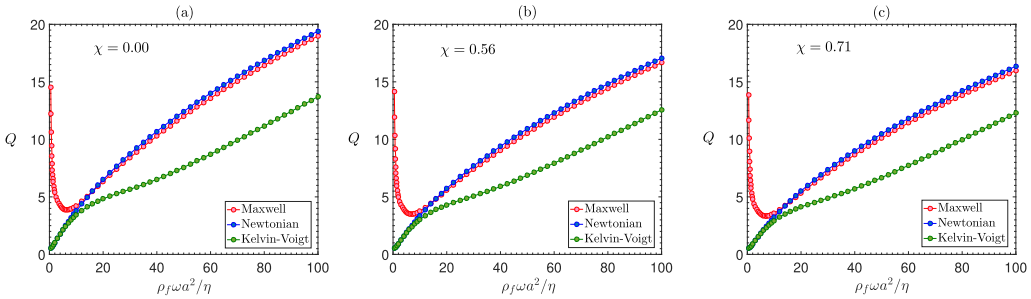

Figure 3. Quality factor versus normalized nanosphere radius.

the Maxwell fluid. If $\chi = 0$ (Figure 2(a)), the numerical results obtained with the Maxwell and Newtonian model converge for each sphere radius. If $\chi = 0.56$ (Figure 2(b)), we can define a pair of critical radius (15 nm and 30 nm). It is seen that the difference between the quality factor values calculated with Newton and Kelvin–Voigt models are negligible if $a < 15$ nm. Otherwise, the quality factor values obtained with the Newtonian model converge toward those obtained with the Maxwell model for $a > 30$ nm. For $a < 15$ nm, the water–glycerol mixture behaves as a viscoelastic solid, and for $a > 30$ nm, the mixture behaves as a viscoelastic fluid. A transition zone appears for $15 < a < 30$ nm. In this range of radius, the quality factor values calculated with Newtonian, Maxwell and Kelvin–Voigt models are different. For if $\chi = 0.71$ (Figure 2(c)), the pair of critical radius is 55 and 100 nm. The Newtonian curve converge toward Kelvin–Voigt curve for $a < 55$ nm and toward Maxwell curve if $a > 100$ nm. It is shown (Figures 2(b) and (c)) that the water–glycerol mixture can be considered as a viscoelastic solid for low radius values and as a viscoelastic liquid for high radius values. These critical radius increase with glycerol concentration.

Instead of plotting the quality factor against the radius (see Figure 2), we can use a non-dimensional normalized radius ($\rho_f \omega a^2/\eta$). Figure 3 illustrates the influence of the normalized nanosphere radius on the quality factor for three glycerol mass fraction $(0, 0.56, 0.71)$. The predicted quality factor by the Newtonian and Kelvin–Voigt models increases with increasing normalized nanosphere radius. A nonmonotonic variation of the quality factor with the normalized radius is observed for the Maxwell fluid. It is seen that the difference between the quality factor values calculated with Newton and Kelvin–Voigt models are negligible if the normalized radius is lower than 12. Otherwise, the quality factor values obtained with the Newtonian model converge toward those obtained with the Maxwell model if the normalized radius is greater than 12.

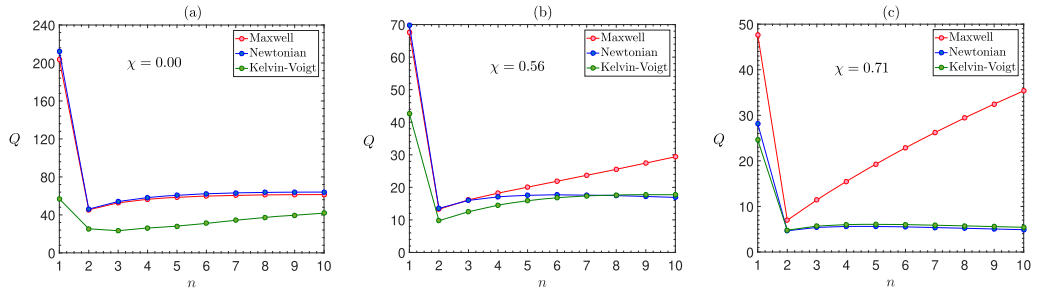

Figure 4. Quality factor as function of angular mode number n.

5.3. *Influence of the angular mode number*

The quality factor of a gold nanosphere vibrating in Newtonian, Maxwell and Kelvin–Voigt fluids as a function of angular mode number n is depicted in Figure 4 for three glycerol mixtures ($\chi = 0, 0.56, 0.71$). One can observe that the quality factor for the purely toroidal mode ($n = 1$) is higher than that of the mode number $n = 2$ (fundamental toroidal mode). According to (17), the numerical results obtained with the Maxwell and Newtonian models converge for $\chi = 0$ (Figure 4(a)). Otherwise, the results obtained with the Kelvin–Voigt and Newtonian models converge for $\chi = 0.71$ (Figure 4(c)). For high glycerol concentration, the mixture behaves as a solid if $\chi = 0.56$ (Figure 4(b)), a pair of critical modes numbers can be defined ($n = 3, 7$). It is shown that the quality factor values calculated with Newtonian model converge to Maxwell ones for $n < 3$ (low frequencies). Otherwise, the Newtonian and Kelvin–Voigt models converge for $n > 7$ (high frequencies). The viscoelastic medium behaves as a viscous fluid for $n < 3$ (low frequencies) and as an elastic solid $n > 7$ (high frequencies).

5.4. *Effect of surrounding fluid on the vibration frequency*

In this paragraph, the effect of surrounding fluid on the vibration frequency is depicted in Figure 5, for an isotropic gold nanosphere submerged in a glycerol–water mixture modeled by a Maxwell fluid. One can observe from Figure 5 that the vibration frequency decreases with the increasing nanosphere radius. Figure 5 also shows that the surrounding fluid has a little effect on the vibration frequency except for small radius values. This indicates that the effect of surrounding fluid on the vibration frequency is more significant when smaller nano-sized spheres are considered. This behavior is also found for Kelvin–Voigt model. Therefore, for radii greater than 18 nm, the vibration frequencies are simply determined using (18) that corresponds to a dry sphere.

6. Conclusion

In this paper, an analytical approach to predict toroidal vibrations of an elastic nanosphere in Newtonian and viscoelastic fluids is proposed. The viscoelasticity is described using Maxwell and Kelvin–Voigt models. The obtained complex eigenvalue equation is first used to study the effect of glycerol concentration on the quality factor of a gold nanosphere vibrating in water–glycerol mixture. A pair of critical concentrations is highlighted and defines three behavior zones: Maxwell, transition and Kelvin–Voigt. In the Maxwell and Kelvin–Voigt domains, the mixture can be considered as a viscous fluid and an elastic solid, respectively. The effect of the sphere radius and mode number on the quality factor was also studied. A pair of critical radius and critical

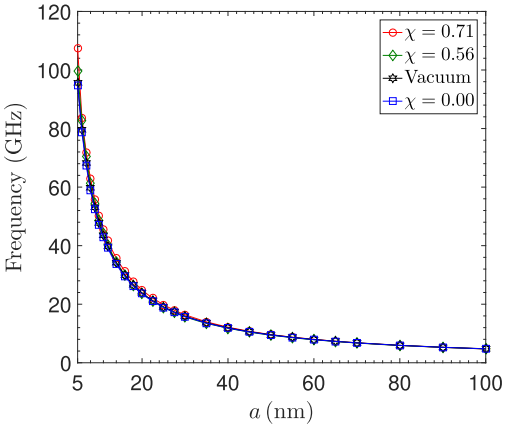

Figure 5. Vibration frequency versus nanosphere radius in the case of Maxwell fluid.

mode numbers are also highlighted. Three behavior zones can also be defined for each glycerol concentration. For low radius or high frequency values the medium can be considered as an elastic solid. For high radius or low frequency values, the medium behaves as a viscous fluid.

Conflicts of interest

The authors declare no competing financial interest.

References

[1] S. S. Verbridge, L. M. Bellan, J. M. Parpia, H. G. Craighead, "Optically driven resonance of nanoscale flexural oscillators in liquid", *Nano Lett.* **6** (2006), p. 2109-2114.

[2] H. Portales, N. Goubet, L. Saviot, S. Adichtchev, D. B. Murray, A. Mermet, E. Duval, M. P. Pileni, "Probing atomic ordering and multiple twinning in metal nanocrystals through their vibrations", *Proc. Natl Acad. Sci. USA* **105** (2008), p. 14784-14789.

[3] K. Jensen, K. Kim, A. Zettl, "An atomic-resolution nanomechanical mass sensor", *Nat. Nanotechnol.* **3** (2008), p. 533-537.

[4] J. L. Arlett, E. B. Myers, M. L. Roukes, "Comparative advantages of mechanical biosensors", *Nat. Nanotechnol.* **6** (2011), p. 203-215.

[5] P. V. Ruijgrok, P. Zijlstra, A. L. Tchebotareva, M. Orrit, "Damping of acoustic vibrations of single gold nanoparticles optically trapped in water", *Nano Lett.* **12** (2012), p. 1063-1069.

[6] D. Chakraborty, E. V. Leeuwen, M. Pelton, J. E. Sader, "Vibration of nanoparticles in viscous fluids", *J. Phys. Chem.* **117** (2013), p. 8536-8544.

[7] M. Babincova, P. Sourivong, P. Babinec, "Resonant absorption of ultrasound energy as a method of HIV destruction", *Med. Hypotheses* **55** (2000), p. 450-451.

[8] L. H. Ford, "Estimate of the vibrational frequencies of spherical virus particles", *Phys. Rev. E* **67** (2003), article no. 051924.

[9] L. Saviot, D. B. Murray, A. Mermet, E. Duval, "Comment on estimate of the vibrational frequencies of spherical virus particles", *Phys. Rev. E* **69** (2004), article no. 023901.

[10] M. Talati, P. K. Jha, "Acoustic phonon quantization and low-frequency raman spectra of spherical viruses", *Phys. Rev. E* **73** (2006), article no. 011901.

[11] S. Sirotkin, A. Mermet, M. Bergoin, V. Ward, J. L. Van Etten, "Viruses as nanoparticles: Structure versus collective dynamics", *Phys. Rev. E* **90** (2014), article no. 022718.

[12] G. V. Hartland, "Coherent excitation of vibrational modes in metallic nanoparticles", *Annu. Rev. Phys. Chem.* **57** (2006), p. 403-430.

[13] M. Fujii, T. Nagareda, S. Hayashi, S. Hayashi, K. Yamamoto, "Low-frequency raman scattering from small silver particles embedded in SiO_2 thin films", *Phys. Rev. B* **44** (1991), p. 6243-6248.

[14] H. Lamb, "On the vibrations of an elastic sphere", *Proc. London Math. Soc.* **13** (1882), p. 189-212.
[15] V. Galstyan, O. S. Pak, H. A. Stone, "A note on the breathing mode of an elastic sphere in Newtonian and complex fluids", *Phys. Fluids* **27** (2015), article no. 032001.
[16] D. Chakraborty, E. Sader, "Constitutive models for linear compressible viscoelastic flows of simple liquids at nanometer length scales", *Phys. Fluids* **27** (2015), article no. 052002.
[17] X. Yang, A. El Baroudi, J. Y. Le Pommellec, "Analytical approach for predicting vibration characteristics of an embedded elastic sphere in complex fluid", *Arch. Appl. Mech.* **90** (2020), p. 1399-1414.
[18] A. El Baroudi, "A note on the spheroidal modes vibration of an elastic sphere in linear viscoelastic fluid", *Phys. Lett. A* **384** (2020), article no. 126556.
[19] W. Abassi, A. El Baroudi, F. Razafimahery, "Torsional vibrations of fluid-filled multilayered transversely isotropic finite circular cylinder", *Int. J. Appl. Mech.* **8** (2016), article no. 1650032.
[20] I. Mnassri, A. El Baroudi, "Vibrational frequency analysis of finite elastic tube filled with compressible viscous fluid", *Acta Mech. Solida Sin.* **30** (2017), p. 435-444.
[21] J. Y. Le Pommellec, A. El Baroudi, "A novel generalized dispersion equation to design circumferential wave fluid sensors", *SN Appl. Sci.* **1** (2019), article no. 788.
[22] D. D. Joseph, *Fluid Dynamics of Viscoelastic Liquids*, Springer, New York, 1990.
[23] P. M. Morse, H. Feshbach, *Methods of Theoretical Physics Part II*, McGraw-Hill, New York, 1946.
[24] M. Pelton, D. Chakraborty, E. Malachosky, P. Guyot-Sionnest, J. E. Sader, "Viscoelastic flows in simple liquids generated by vibrating nanostructures", *Phys. Rev. Lett.* **111** (2013), article no. 244502.
[25] T. A. Major, A. Crut, B. Gao, S. S. Lo, N. D. Fatti, F. Vallee, G. V. Hartland, "Damping of the acoustic vibrations of a suspended gold nanowire in air and water environments", *Phys. Chem. Chem. Phys.* **15** (2013), p. 4169-4176.
[26] L. Saviot, D. B. Murray, A. Mermet, E. Duval, "Damping by bulk and shear viscosity of confined acoustic phonons for nanostructures in aqueous solution", *J. Phys. Chem. B* **111** (2007), p. 7457-7461.